The Journal of Immunology



# A Novel Leukocyte Adhesion Deficiency III Variant: Kindlin-3 Deficiency Results in Integrin- and Nonintegrin-Related Defects in Different Steps of Leukocyte Adhesion

Philippe Robert, Matthias Canault, Catherine Farnarier, Alan Nurden, Charlotte Grosdidier, Vincent Barlogis, Pierre Bongrand, Anne Pierres, Hervé Chambost and Marie-Christine Alessi

*J Immunol* 2011; 186:5273-5283; Prepublished online 25 March 2011;
doi: 10.4049/jimmunol.1003141
http://www.jimmunol.org/content/186/9/5273



*The Journal of Immunology* is published twice each month by
The American Association of Immunologists, Inc.,
1451 Rockville Pike, Suite 650, Rockville, MD 20852

Print ISSN: 0022-1767 Online ISSN: 1550-6606.

# A Novel Leukocyte Adhesion Deficiency III Variant: Kindlin-3 Deficiency Results in Integrin- and Nonintegrin-Related Defects in Different Steps of Leukocyte Adhesion

**Philippe Robert,[*,†,‡,§] Matthias Canault,[†,¶] Catherine Farnarier,[*] Alan Nurden,[‖] Charlotte Grosdidier,[†,¶,#] Vincent Barlogis,[**] Pierre Bongrand,[*,†,‡,§] Anne Pierres,[†,‡,§] Hervé Chambost,[†,¶,**] and Marie-Christine Alessi[†,¶,#]**

**Leukocyte adhesion deficiency type III is a recently described condition involving a Glanzmann-type bleeding syndrome and leukocyte adhesion deficiency. This was ascribed to a defect of the *FERMT3* gene resulting in abnormal expression of kindlin-3, a protein expressed in hematopoietic cells with a major role in the regulation of integrin activation. In this article, we describe a patient with a new mutation of *FERMT3* and lack of kindlin-3 expression in platelets and leukocytes. We assayed quantitatively the first steps of kindlin-3–defective leukocyte adhesion, namely, initial bond formation, bond strengthening, and early spreading. Initial bond formation was readily stimulated with neutrophils stimulated by fMLF, and neutrophils and lymphocytes stimulated by a phorbol ester or $Mn^{2+}$. In contrast, attachment strengthening was defective in the patient's lymphocytes treated with PMA or $Mn^{2+}$, or fMLF-stimulated neutrophils. However, attachment strengthening was normal in patient's neutrophils treated with phorbol ester or $Mn^{2+}$. In addition, the patient's T lymphocytes displayed defective integrin-mediated spreading and a moderate but significant decrease of spreading on anti-CD3–coated surfaces. Patient's neutrophils displayed a drastic alteration of integrin-mediated spreading after fMLF or PMA stimulation, whereas signaling-independent $Mn^{2+}$ allowed significant spreading. In conclusion, the consequences of kindlin-3 deficiency on $\beta_2$ integrin function depend on both cell type and the stimulus used for integrin activation. Our results suggest looking for a possible kindlin-3 involvement in membrane dynamical event independent of integrin-mediated adhesion.** ***The Journal of Immunology*****, 2011, 186: 5273–5283.**

Integrins are prominent adhesion receptors including 24 different αβ heterodimers formed between 18 α-chains and 8 β-chains (1). $\beta_2$ integrins are expressed by leukocytes, and $\alpha_L\beta_2$ (also called CD11aCD18 or LFA-1) mediates adhesion to ICAM ligands, particularly the ubiquitous ICAM-1/CD54 carried by endothelial cells and leukocytes. LFA-1 mediates leukocyte–endothelium adhesion, and participates in transmigration and leukocyte–leukocyte interactions during immune responses (2). Another integrin, $\alpha_{IIb}\beta_3$ (also called GPIIb-IIIa), is important in allowing platelets to bind fibrinogen and promotes clotting (3).

Many integrins are inactive on resting cells. Different cell stimuli can activate integrin function by triggering inside-out signaling (1, 4). This activation is a multistep process involving conformational changes with increased accessibility and affinity of the ligand-binding site. Also involved are integrin clustering (5) and interaction with cytoskeletal elements (6). These changes influence integrin diffusion velocity (7, 8) and association with cell surface-bound ligands. Integrin–ligand interactions trigger outside-in signaling cascades, thus altering cell function. Integrins are thus bidirectional signaling machines (9). Integrin activation and signal generation therefore involve a complex network of molecular interactions (2, 10). Specific defects of integrin regulatory molecules may help us understand integrin function. Conversely, diagnosis of these defects may benefit from assays developed for understanding integrin function.

During the last decade, leukocyte adhesion deficiency type III (LAD-III) was reported in patients of mostly Turkish (11–13), but also Arab (12, 14), Maltese (13), or African American (15) origin. Mutations within the *FERMT3* gene prevented kindlin-3 expression. This protein is expressed in hematopoietic cells and binds the β subunit of integrins by interacting with the C-terminal NXXY/F site. This interaction stabilizes active conformations of the integrin subunits (1, 4, 16). Kindlin-3 deficiency was reported to cause abnormal β integrin activation. Defective function of $\beta_3$ integrin causes a bleeding defect as observed in Glanzmann thrombasthenia. Defective activation of $\beta_2$ integrins may generate

*Laboratoire d'Immunologie, Hôpital de la Conception, Assistance Publique-Hôpitaux de Marseille, 13385 Marseille Cedex 05, France; [†]Université de la Méditerranée, 13284 Marseille Cedex 07, France; [‡]INSERM Unité Mixte de Recherche 600, 13288 Marseille Cedex 09, France; [§]Centre National de la Recherche Scientifique Unité Mixte de Recherche 6212, 13288 Marseille Cedex 09, France; [¶]INSERM Unité Mixte de Recherche 626, 13385 Marseille Cedex 05, France; [‖]Centre de Référence sur les Pathologies Plaquettaires, Hôpital Xavier Arnozan, 33604 Pessac, France; [#]Laboratoire d'Hématologie, Hôpital de la Timone, Assistance Publique-Hôpitaux de Marseille, 13385 Marseille Cedex 05, France; and **Service d'Hématologie Pédiatrique, Hôpital de la Timone, Assistance Publique-Hôpitaux de Marseille, 13385 Marseille Cedex 05, France

Received for publication September 21, 2010. Accepted for publication February 28, 2011.

This work was supported by INSERM (ANR-08-GENO-028-03) and Groupement d'Intérêt Scientifique-Maladies Rares.

Address correspondence and reprint requests to Dr. Pierre Bongrand, Laboratoire d'Immunologie, Hôpital de la Conception, 147 Boulevard Baille, 13385 Marseille Cedex 05, France. E-mail address: pierre.bongrand@inserm.fr

The online version of this article contains supplemental material.

Abbreviations used in this article: IRM, interference reflection microscopy; LAD-I, leukocyte adhesion deficiency type I; LAD-III, LAD type III; MFI, mean fluorescent intensity; PRP, platelet-rich plasma; RICM, reflection interference contrast microscopy.



www.jimmunol.org/cgi/doi/10.4049/jimmunol.1003141

an immune deficiency that is, however, milder than in type I LAD (LAD-I) involving a lack of $\beta_2$ integrin expression.

In this article, we describe the integrin-dependent cell functions of a patient of gypsy origin carrying both a heterozygous mutation of the integrin $\alpha_{IIb}$ (*ITG2B*, *CD41B*) and a new homozygous mutation of *FERMT3*. This patient suffers from an LAD-III syndrome with a serious bleeding defect and immune deficiency. To dissect the abnormality of integrin function, we subjected the patient's leukocytes to specific tests to quantify three early steps of LFA-1 interaction with ICAM-1 ligand. This approach allowed us to localize the functional deficiency of the patient's neutrophils and lymphocytes. Interestingly, functional defects were dependent on cell type (neutrophil versus T lymphocyte), as well as the stimulus used for integrin activation (chemotactic peptide versus phorbol ester). Unexpectedly, a spreading defect was found in an integrin-independent process, suggesting an additional role for kindlin-3. Accurate dissection of the early steps of integrin-mediated adhesion will give a greater insight into the mechanisms of integrin activation and intracellular signaling cascades.

## Materials and Methods

Investigations were performed in accordance with the Declaration of Helsinki. Written informed consent was obtained from the patient's parents. All control subjects gave informed consent in accordance with the Declaration of Helsinki.

### *Molecular biology*

DNA was isolated from blood collected in EDTA tubes by the salting-out method. *FERMT3* 15 exons were amplified by PCR in 11 amplicons on a Biometra thermal cycler (Labgene Scientific Instruments, Archamps, France). PCR products were purified by filtration using a cleanup kit (Millipore, Billerica, MA) and run on agarose gel for quantification by comparison with DNA ladders (Fermentas, Burlington, ON, Canada). Purified PCR products were sequenced by Cogenics, France; sequences were visualized using Chromas Lite 2.01 free software and aligned using Multialign free software.

Total RNA was isolated from blood collected on EDTA tubes using QIAamp RNA Blood kit (Qiagen, Courtaboeuf, France), quantified using a Nanodrop spectrometer (Thermo Fisher Scientific, Waltham, MA), and reverse transcribed using M-MLV reverse transcriptase (Invitrogen, Cergy Pontoise, France), following the manufacturer's protocols. The first 1817 of *FERMT3* mRNA 2558 bp were amplified in 5 overlapping amplicons and sequenced as described earlier. cDNA sequence analysis was performed as described earlier.

Real-time quantitative PCR was performed after extracting total RNA from platelet samples with QIAamp RNA mini kit (Qiagen) as recommended by the manufacturer. cDNAs were retrotranscribed from 1 μg total RNA, using M-MLV reverse transcriptase and RNase inhibitor (Invitrogen, San Diego, CA), as recommended by the manufacturer. Quantitative PCR was conducted on a LightCycler-480 II instrument (Roche Applied Bioscience, Manheim, Germany), using SYBR Green dye (Roche). The relative amount of *FERMT3* mRNA was normalized to GAPDH mRNA level and expressed relatively to the value obtained for the control subject (user bulletin 2; Applied Biosystems, Foster City, CA). Presented values were obtained from two separate experiments realized in duplicate and are expressed as mean ± SEM.

### *Platelet studies*

*Platelet preparation.* Blood from the LAD-III patient, his mother and father, or healthy volunteers was collected in buffered citrate (0.105 M). Whole blood was centrifuged at 200 × *g* for 10 min to prepare platelet-rich plasma (PRP).

*Flow cytometry.* PRP was diluted 1/10 in Tyrode's albumin buffer ($0.25 \times 10^8$/ml) and gently mixed. Abs to CD41/CD61 (clone P2), CD42b/CD42d/CD42a (clone SZ1) were from Beckman Coulter (Villepinte, France), and Ab directed against the active form of GPIIb-IIIa (clone PAC-1) from BD Biosciences (Erembodegem, Belgium). Ten microliters diluted PRP was incubated with ADP (final concentration, 10 μM), TRAP-6 (final concentration, 50 μM), or Tyrode's albumin buffer. After 30-min incubation, 10 μl FITC-labeled goat $F(ab')_2$ anti-mouse IgG+IgM (diluted 1/10) was added. Scatter signals and fluorescence intensity were analyzed using an FC500 flow cytometer (Beckman Coulter).

*Platelet aggregation.* PRP was diluted with platelet-poor plasma to achieve a platelet concentration of $3 \times 10^8$/ml. Diluted PRP was placed in an aggregometer cuvette at 37°C and stirred. Agonists were added and light transmission was recorded for 10 min on an APACT 4004 optical aggregation system (Labor BioMedical Technologies GmbH, Ahrensburg, Germany).

### *Leukocyte studies*

*Leukocyte preparation.* Leukocytes from control subjects (blood bank), a previously explored LAD-I patient, and the propositus were obtained by centrifugation on a density barrier (MSL; Eurobio, Les Ulis, France). T lymphocytes were purified from PBMCs by negative selection, using magnetic cell sorting with microbeads coated with anti–HLA-DR Abs (Miltenyi Biotec, Bergisch Gladbach, Germany). This yielded T lymphocytes mixed with 10–15% NK cells. In some experiments, similar results were obtained with *Pan* T isolation kit II (Miltenyi Biotec), yielding nearly 100% T lymphocytes. Sedimented granulocytes were purified by 30-s hypotonic shock.

*Flow cytometry.* Leukocyte counts and surface glycoprotein expression were assessed on a Canto II flow cytometer (BD Biosciences) and an EPICS XL flow cytometer (Beckman Coulter). Abs used for membrane glycoproteins were monospecific for CD11a, CD11b, CD18, CD15, E selectin, CD29 (all reagents from Beckman Coulter), and CD11c (Dako, Glostrup, Denmark). Abs used for leukocyte counts were CD3, CD4, CD8, CD16, CD29, CD45 RA, CD45 RO, CD56 (BD Biosciences). mAb 24, which was shown to be specific for an active conformation of the leukocyte integrin α subunits (17), was used as follows: leukocytes were incubated for 30 min in stimulation medium as described later; then they were incubated for 30 min with 10 μg/ml mAb 24 (Abcam, U.K.) or control isotype. Cells were then rinsed twice in PBS, then incubated at room temperature with 10 μg/ml FITC-labeled goat anti-mouse $F(ab')_2$ (Beckman Coulter) and immediately analyzed with a Canto II flow cytometer. Results were expressed as specific binding by subtracting the fluorescence of cells treated with control Ig of matched isotype from the fluorescence of cells treated with mAb 24.

*Neutrophil phagocytic activity and oxidative burst.* Phagocytosis and oxidative burst were assayed as previously described (18). In brief, cells were allowed to phagocytose serum-opsonized zymosan particles. The oxidative burst was assayed by incubating cells with either zymosan, 50 ng/ml PMA, a protein kinase C activator (Sigma-Aldrich, St. Louis, MO), or 1 μM fMLF (a chemoattractant mimicking some bacterial proteins; Sigma-Aldrich) and 80 μM ferricytochrome *c* (Sigma-Aldrich). Ferricytochrome *c* reduction was assayed by spectrophotometry.

*Lymphocyte proliferation assays.* PBMCs were fractionated from EDTA- or heparin-anticoagulated venous blood and stained with CFSE (Invitrogen). CFSE fluorescence intensity was measured by flow cytometry; then cells were placed in 96-well microplates (Thermo Fisher Scientific), in RPMI 1640 medium supplemented with 20 mM HEPES, 10% FCS, 2 mM L-glutamine, 50 U/ml penicillin, and 50 U/ml streptomycin (all products from Invitrogen). Proliferation was induced with either CD3 (Beckman Coulter), PHA A (Thermo Fisher Scientific), or PWM (Sigma-Aldrich). Stimulation for Ag proliferation assays was done with either candidin (Bio-Rad, Richmond, CA), tuberculin, or tetanus toxin (Sanofi Aventis, Paris, France). Each assay was done in triplicate; a proliferation assay with cells from a healthy donor was performed in parallel as a positive control. Cells were recovered after 4 d of culture; for each stimulation, cells were stained with phycocyanin-5–conjugated CD3 (Beckman Coulter), or propidium iodide (Invitrogen), or kept without staining. CFSE fluorescence intensity was measured by flow cytometry. Data were analyzed with FACSDiva software (BD Biosciences).

*Integrin capacity to bind soluble ligands.* Soluble ICAM-1 binding assays were performed using a Canto II flow cytometer (BD Biosciences, France). T lymphocytes were stained with PE-conjugated anti-CD3 (BD Biosciences, France) or PE-conjugated isotype control Ab. Cells were simultaneously incubated with Fc-ICAM (R&D Systems) and FITC-conjugated anti-human Fc mouse Ab (BD Biosciences, France) or FITC-conjugated anti-human Fc mouse Ab alone for controls. Staining, washing, and flow cytometry assays were done either in 0.9% NaCl solution (Biosedra, Fresenius-Kabi, France) buffered with 25 mM HEPES (Invitrogen, France) and 10 mM $Mn^{2+}$ (Sigma-Aldrich, France) for integrin activation, or in 0.9% NaCl solution buffered with 25 mM HEPES and 10 mM EDTA (Sigma-Aldrich, France) for integrin inhibition.

*Laminar flow adhesion assay.* The use of a flow chamber operated under low shear rate for adhesion assays was fully described by us previously (19, 20). Leukocytes were driven through parallel-plate channels of 2 mm in width and 0.1 mm in height. The bottom surface was a glass coverslip coated

with ~200 Fc-ICAM molecules/$\mu m^2$. Wall shear rate was ~20 $s^{-1}$, thus subjecting surface-bound cells to a viscous force of the order of 7 pN (21). Thus, a single molecular bond could generate a detectable cell arrest with a typical duration of the order of 1 s. Control experiments confirmed that binding events were fully blocked by an excess of soluble anti–ICAM-1 Abs (not shown). Images were acquired with a video camera (HyperHAD; Sony France, Clichy, France) on an Olympus IX 50 inverted microscope set within a closed box maintained at 37°C. Pixel size was $1 \times 1$ $\mu m^2$ with a 10× objective. Sequences of typically 4-min duration were digitized and DivX compressed with a Win-TV digitizer (Hauppauge, France) for delayed analysis. Cell trajectories were tracked along paths of 565-μm average length, and the number of detectable arrests (duration longer than ~200 ms) and the number of permanent arrests (i.e., arrests lasting >2 min) were quantified. In some experiments, cells were stimulated for 15 min at 37°C with 1 μM fMLF or 100 ng/ml PMA. In other experiments, integrin activation was achieved by adding 10 mM $MnCl_2$ in the medium used for adhesion experiments.

*Membrane alignment assay.* The assay consisted of using interference reflection microscopy (IRM), also called reflection interference contrast microscopy (RICM), to measure the area of molecular contacts formed between leukocytes and surfaces prepared with Abs specific for cell surface molecules or integrin ligands (anti-CD3, anti-HLA Abs recognizing a nonpolymorphic epitope of HLA-A, HLA-B, and HLA-C, or ICAM-1). Twenty microliters of lymphocyte suspensions ($12.5 \times 10^6$/ml) was rapidly added near the bottom of custom-made chambers (shaped as cylinders of 5-mm height, 1-$cm^2$ basis area). The lower surface of the chambers was a glass coverslip bearing ~300 adhesion molecules/$\mu m^2$. Chambers were then incubated for 15 min at 37°C on the stage of a Zeiss Axiovert 135 inverted microscope bearing a heating stage (TRZ 3700) set at 37°C. Cells were then examined with IRM as previously described (22, 23). Typically, series of 10 microscope fields were then rapidly recorded with a Hamamatsu Orca C4742-45-10 video camera yielding 10-bit accuracy. Pixel size was $125 \times 125$ $nm^2$. Images were processed quantitatively to determine the membrane-surface distance with a resolution better than 5 nm. Contact areas were defined as regions where the apparent membrane-to-surface distance was less than ~34 nm (22, 23). About 100 cells were examined under each tested condition to calculate the mean contact area per cell. It was previously shown that lymphocytes deposited on anti-CD3, not anti-HLA, started proliferating (23). When cells were deposited on surfaces coated with irrelevant Ig, no molecular contact area was detected (not shown).

### *Immunoblot analysis*

*Platelet lysis.* PRP was centrifuged at $1000 \times g$ for 5 min. Platelets were lysed with T3EN-SDS-*N*-ethylmaleimide buffer (10 mM Tris-HCl, 150 mM NaCl, 3 mM EDTA, 6 mM *N*-ethylmaleimide, 2.5% $NaDodSO_4$ [SDS], pH 7.00) containing serine-protease inhibitors Pefabloc SC (Sigma-Aldrich).

*Lymphocyte lysis.* Pelleted cells were lysed with RIPA buffer (Sigma-Aldrich) containing Pefabloc SC (Sigma-Aldrich). Total protein from the cell lysates was assayed using the Bicinchoninic Acid Kit for protein determination (Sigma-Aldrich). Samples (30 μg protein) were separated by SDS-PAGE and transferred onto a polyvinylidene difluoride membrane. Individual proteins were detected with mAbs against kindlin-3 (URP2; Abcam, Cambridge, MA), CalDAG-GEF-I (RASGRP2; Abcam), talin (Novus Biological, Littleton, CO), and polyclonal Ab against human β-actin (Sigma-Aldrich). Secondary Abs were either a goat anti-rabbit or anti-mouse Ig HRP coupled (Bio-Rad). Proteins were visualized by ECL.

### *Statistical analysis*

Confidence intervals and comparison with Student *t* test were performed with Excel software. Comparison between frequencies (Table I) was performed on the basis of the binomial law (24).

## Results

### *Patient history*

The patient, a 33-mo-old boy, was born by assisted labor after an uneventful pregnancy. He was the first child of a consanguineous marriage of gypsy ethnicity; the family history was unremarkable.

At delivery, physical examination revealed petechial bleeding attributed to the traumatic delivery as laboratory studies revealed a normal platelet count and normal coagulation tests (prothrombin time, activated partial prothrombin time). However, 2 mo later, the patient's purpura had returned and he was hospitalized. His hemoglobin level was 97 g/dl, and his hematocrit was 0.30%. Levels of clotting factors, von Willebrand factor, plasminogen activator inhibitor-1, α2 antiplasmin, and factor XIII were normal. The PFA-100 (Dade Behring, Miami, FL) occlusion times for the Col-Epi and Col-ADP cartridges were prolonged to 210 and 209 s (reference ranges: 80–160 and 59–120 s, respectively). His platelet count was 277 g/l, and mean platelet volume was 10.4 fl. Platelet aggregation testing on several occasions revealed that platelets failed to aggregate in response to ADP, epinephrine, collagen, calcium ionophore (A23187), and TRAP. However, ristocetin-induced aggregation was normal (data not shown).

At the age of 5 mo, the patient presented a severe pneumopathy with dyspnea and hypoxia. WBC count was 65 g/l (30 g/l neutrophils, 30 g/l lymphocytes, and 1.8 g/l monocytes). Microbiological testing of sputum failed to reveal any pathogen including *Pneumocystis jiroveci*. Treatment with wide-spectrum antibiotic therapy and cotrimoxazole was initiated, and the pulmonary symptoms resolved in a few days. At the same time, a reduced level of Ig was discovered: IgG/M/A: 1.5/0.23/0.08 g/l (reference ranges: 2.3–4.3/0.3–0.9/0.2–0.6 g/l, respectively). An inherited immunodeficiency was suspected and the child received a long-term prophylaxis based on the association of antibiotics with cotrimoxazole, itraconazole, and Ig replacement therapy. Despite this treatment, WBC leukocyte counts were constantly increased even in the absence of infection and with normal C-reactive protein levels. The WBC differential counts monitored over a 30-mo period demonstrated that, in addition to neutrophils (mean ± SD [5–95th]: 11 ± 5.9 [3.5–25] g/l; $n = 39$), total lymphocytes were also elevated (mean ± SD [5–95th]: 16 ± 6.9 [1.6–30]; $n = 39$). At 33 mo, the child has a normal statural growth and neuropsychological development. The bleeding tendency has continued with long-lasting mucocutaneous impairment and frequent bruising. A more serious bleeding episode involving a penis hematoma was resolved by giving recombinant activated factor VII. Repeated clinical examination revealed a transient hepatosplenomegaly. X-ray films of long bones did not show evidence of osteopetrosis. Examination of the parents did not reveal any clinical or biological abnormality.

### *Platelet studies revealed a Glanzmann-like functional defect*

The patient's platelets failed to aggregate with all physiologic agonists tested (see *Patient history* earlier in this article and Supplemental Fig. 1). Flow cytometry analysis showed a comparable GPIIb-IIIa expression with that of his mother (mean fluorescent intensity [MFI]: 22.6 versus 28.1) but lower than that of his father (MFI: 51). Strikingly, the patient's platelets were unable to unmask activation-dependent epitopes on GPIIb-IIIa, because binding of PAC-1 Ab was not increased after ADP or TRAP stimulation (MFI, mean ± SD: 2.33 ± 0.54 and 1.8 ± 0.01, respectively), compared with reference values (reference ranges [min-max]: 5.4–16 and 3.9–9, respectively). However, when inside-out signaling was bypassed using 1 mM $MnCl_2$ to directly activate GPIIb-IIIa, platelet aggregation was at least partially restored (Supplemental Fig. 1). Taken together, these results indicate that the GPIIb-IIIa activation signaling cascade is defective in the patient's platelets, suggesting that he was a Glanzmann thrombasthenia variant (25). However, sequencing (Fig. 1) of the coding regions and splice sites of the *ITGA2B* and *ITGB3* genes demonstrated that the patient and his mother, but not his father, were heterozygous for the 1544+1G>A transition in intron 15 of the *ITGA2B* gene, a well-characterized mutation that leads to a frameshift and stop codon, and an absent GPIIb-IIIa expression

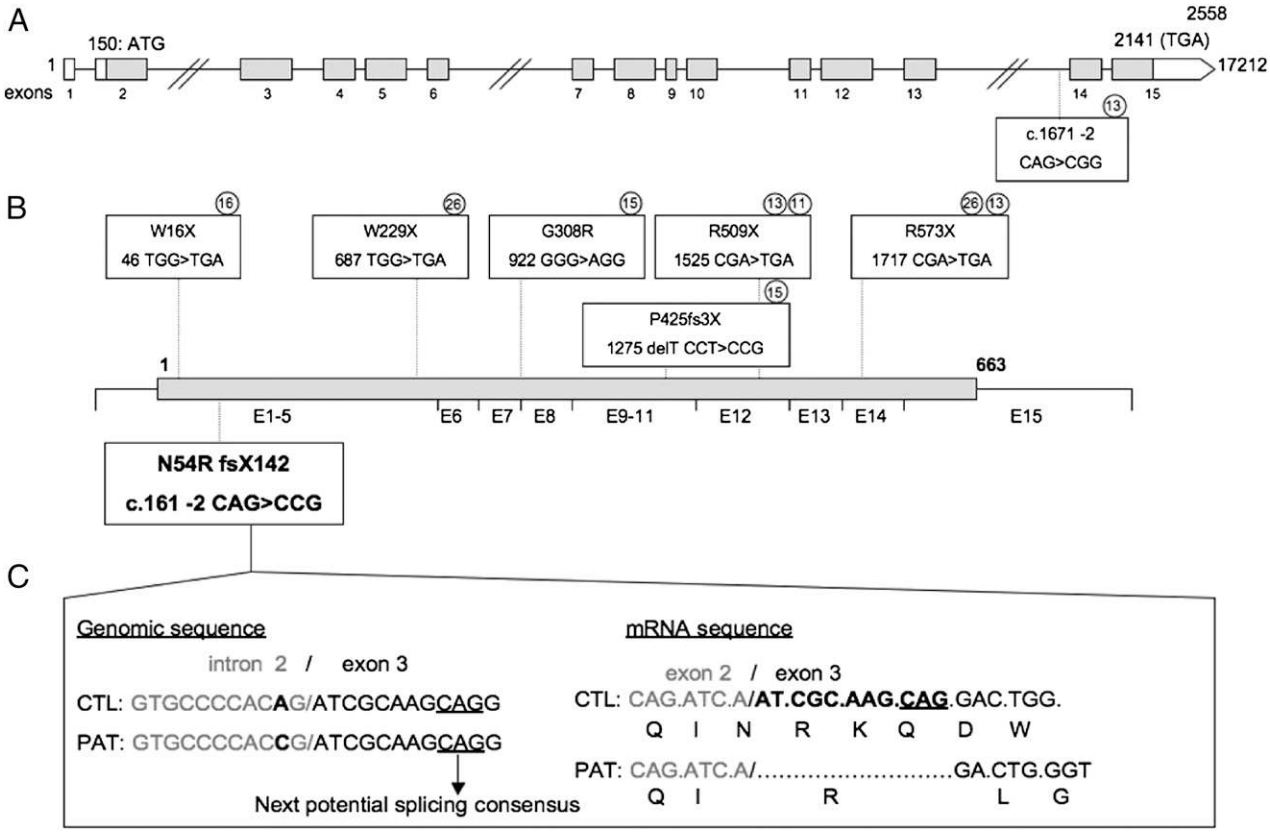


**FIGURE 1.** FERMT3 gene structure and reported mutations. *A*, Schematic representation of the FERMT3 gene structure: exons are depicted as rectangles with corresponding numbering underneath; mRNA numbering above (from clone NM_031471); genomic numbering at the extremities. *B*, Coding sequence along with exon position and published mutations. E represents exon; numbering is for amino acid sequence (short form, NP_113659). Published mutations are denoted as amino acid (first line) and nucleotide (second line). C.1671-2 affects exon 14 splicing consensus sequence and generates a variety of aberrant spliced products but no protein. *C*, Detailed sequence for the new mutation reported. The mutation in the genomic sequence is in bold. The aberrantly spliced sequence at the mRNA level is depicted in bold, and the corresponding amino acid sequence is under the two different mRNA sequences. CTL, control sequence; PAT, patient sequence (heterozygous parents are not represented).

in the French gypsy population of Manouche origin (26). No other potential mutations were present that could account for the altered function of the residual GPIIb-IIIa in his platelets.

Table I. Comparison of adhesion receptors on control subjects' and patient's blood cells

| Adhesion Molecule | Cell Type | Control Subject % Positive | Control Subject Median | Patient % Positive | Patient Median |
|---|---|---|---|---|---|
| CD11a | Lymphocytes | 92 | 2.5 | 90 | 1.2 |
| | Monocytes | 95 | 6.1 | 96 | 3.8 |
| | Neutrophils | 100 | 1.4 | 96 | 1 |
| CD11b | Lymphocytes | 21 | 0.9 | 15 | 1.5 |
| | Monocytes | 95 | 14 | 68 | 4.5 |
| | Neutrophils | 100 | 5.7 | 97 | 1.7 |
| CD11c | Lymphocytes | 13 | 0.5 | 26 | 0.4 |
| | Monocytes | 98 | 4.0 | 92 | 2.5 |
| | Neutrophils | 93 | 1.1 | 53 | 0.7 |
| CD18 | Lymphocytes | 98 | 2.6 | 85 | 0.9 |
| | Monocytes | 100 | 18.3 | 99 | 5.2 |
| | Neutrophils | 100 | 5.3 | 99 | 1.9 |
| CD29 | Lymphocytes | 45 | 1.4 | 13 | 1.3 |
| | Monocytes | 94 | 7.0 | 95 | 2.3 |
| | Neutrophils | 41 | 1.5 | 10 | 0.7 |
| CD62L | Lymphocytes | 30 | 0.6 | 75 | 2.0 |
| | Monocytes | 22 | 1.2 | 62 | 2.1 |
| | Neutrophils | 45 | 0.8 | 79 | 1.7 |

Blood cell populations from patient and a healthy control subjects were assayed with flow cytometry. The fraction of positive cells and median fluorescence are shown.

*Immunological investigations showed a moderate immune deficiency with a decrease of lymphocyte proliferation and Ig production*

Flow cytometry did not reveal any notable alteration of adhesion receptor expression (Table I). In addition to the aforementioned persistent hypogammaglobulinemia, lymphocyte proliferation was markedly decreased after stimulation with anti-CD3 Abs, whereas the responses to PHA or PWM were not altered. Proliferative response to candidin was absent, whereas the response to tetanus toxoid was normal (not shown). In contrast, neutrophil function (Table II), as well as NK and Ab-dependent cytotoxicity, was normal (not shown). A noticeable finding is that the oxidative

Table II. Phagocytic and oxidative activity of patient's neutrophils

| | Patient | Control Samples |
|---|---|---|
| Phagocytosis | | |
| Fraction of cells having phagocytosed | 0.15 | 0.22 (0.095 SD) |
| Ingested particles per phagocytic cell | 2.6 | 2.80 (0.92 SD) |
| Oxidative burst (nmol $O_2^-$ per million of cells per min) | | |
| Stimulation | | |
| fMLF | 63.2 | 28.5 (21.5 SD) |
| PMA | 89.1 | 36.4 (16.9 SD) |
| Zymosan | 14.7 | 10.7 (6.3 SD) |

Patient's neutrophils were assayed for phagocytosis of zymosan particles and superoxide production after stimulation with fMLF, PMA, or zymosan. Results are shown together with mean values obtained on 40 (phagocytosis) or 67 (oxidative burst) samples.

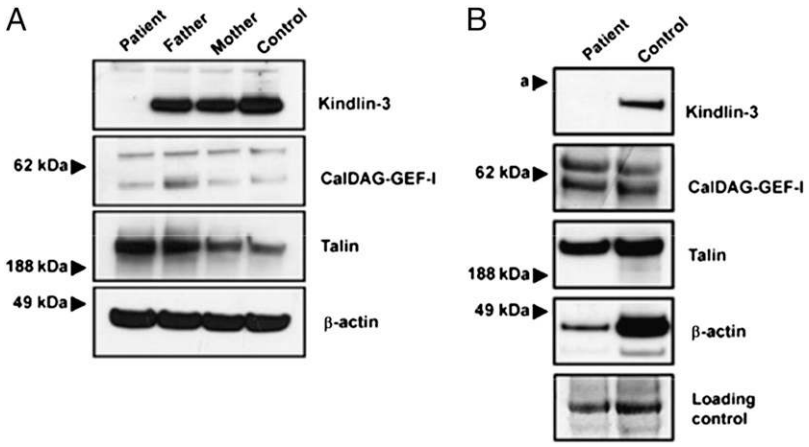


**FIGURE 2.** Western blot analysis of cells from LAD-III patient and control subjects. Western blot analysis of Kindlin-3, CalDAG-GEF-I, talin, and β-actin expression from washed platelet (*A*) and lymphocytes (*B*). Results are representative of three separate Western blot analysis.

burst measured on the patient's neutrophils was comparable with the highest control values for all tested stimuli.

In view of recent reports, the combination of a moderate immune deficiency and a more severe Glanzmann-like bleeding tendency was suggestive of an LAD-III (27) due to a lack of kindlin-3 resulting from a homozygous mutation of the *FERMT3* gene. This was an incentive to sequence *FERMT3* in our patient.

### *Molecular studies identified a new mutation of FERMT3 gene resulting in a lack of kindlin-3 in patient's platelets and leukocytes*

The patient showed a single homozygous base change that does not correspond to any known polymorphism in the *FERMT3* gene. His mother and his father both showed heterozygosity for the mutation. Sequencing the 15 exons and the intron/exon boundaries of the *FERMT3* gene of the patient and his parents yielded no further mutation.

The homozygous mutation was detected in the acceptor splicing site consensus located right before exon 3 (Fig. 1), which begins at nt 310 when considering clone NM_031471, and is described as follows: c.310-2A>C. RNA was then checked for splicing changes. Alignments show the use of a cryptic splice site 10 nt after the normal start of exon 3, resulting in a shift in the open reading frame (p.Asn54ArgfsX142). Parents were confirmed as heterozygous carriers.

Quantitative real time-PCR revealed that the patient's platelets expressed approximately half the level of *FERMT3* mRNA as compared with control platelets. Levels of mRNA for the parents were indistinguishable from those of the control subject (relative expression compared with the control subject: father, 1.03 ± 0.11; mother, 0.95 ± 0.21; patient, 0.42 ± 0.21).

Because mutations in the CalDAG-GEF-I gene have been previously suspected to be responsible for the LAD-III disorder (27), we also analyzed the CalDAG-GEF-I (*RASGRP2*) genomic DNA and cDNA sequence from the patient's leukocytes. We did not find any alteration in the sequence of the CalDAG-GEF-I gene.

To confirm the lack of expression of kindlin-3 in the patient's cells, we then investigated the levels of kindlin-3 protein in platelets and lymphocytes from the patient by Western blot (Fig. 2*A* and 2*B*, respectively). No kindlin-3 protein was detected for the patient, whereas it was readily detectable in his parents' cells. The expression of talin and CalDAG-GEF-I was found to be normal in all family members.

Taken together, these results confirm that the LAD-III disorder is due to a mutation in the *FERMT3* gene causing the absence of a normal kindlin-3 protein in platelets and lymphocytes. As a result, the integrins failed to activate, causing impaired platelet and leukocyte integrin-dependent function.

In view of the present interest in integrin regulation (1, 4) and kindlin-3 function (16), we next analyzed in more detail integrin-mediated leukocyte adhesion.

### *Leukocyte adhesion under flow*

Although flow chambers have long been used with a wall shear rate of the order of 100 $s^{-1}$ to mimic leukocyte–endothelium interaction in blood vessels, we have previously shown that they provide a highly sensitive means of detecting individual bond formation and rupture provided they are operated with a shear rate of the order of 10 $s^{-1}$ in association with an image processing system allowing the detection of events of a few tens of millisecond duration (19, 28). This method was used to study the capacity of LAD-III leukocytes to bind to surfaces coated with the LFA-1 ligand ICAM-1.

*Granulocyte adhesion.* Patient's cells displayed numerous transient arrests, with a frequency comparable with that found for four separate controls (Fig. 3*A*). After fMLF stimulation, the frequency of arrests increased in both the patient and control cells. Interestingly, chemoattractant stimulation induced a marked strengthening of initial arrests in controls (4.3-fold increase), but not in the patient's cells (Fig. 3*B*).

In contrast, PMA increased both LAD-III (2.2-fold increase) and control cell (2.8-fold increase) adhesion, and adhesion strengthening was dramatically increased (≈10-fold or more) in both samples. Finally, when manganese was used to induce integrin activation in a signaling-independent way, both patient's and control subjects' cells displayed increased adhesion frequency and adhesion strengthening. The dominant role played by $\beta_2$ integrins in our adhesion assay is supported by the lack of LAD-I cell adhesion under all tested experimental conditions.

*Lymphocyte adhesion.* Although T lymphocytes from the patient displayed similar adhesion frequency and adhesion strengthening to control subjects in the absence of stimulation, PMA induced 2-fold lower adhesion frequency in patient's cells (Fig. 4*A*; $p < 0.003$) and failed to increase adhesion strengthening in cells from the patient (Fig. 4*B*). Finally, manganese strongly increased adhesion efficiency in both LAD-III cells and controls, and manganese provoked a similar 6-fold enhancement of soluble ICAM uptake by both control and patient lymphocytes (Table III).

Taken together, these results show that kindlin-3 deficiency did not impair the integrin capacity to increase initial binding rate in response to inside-out signaling cascades triggered by fMLF or PMA. However, results support the view that kindlin-3 is partly

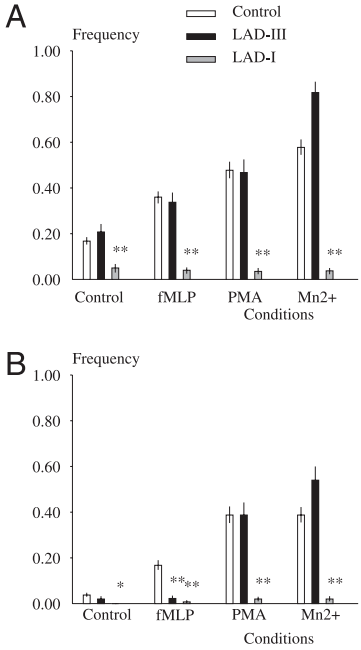


**FIGURE 3.** Neutrophil adhesion under flow. Neutrophils from control (white bars), LAD-III (black bars), or from another patient with LAD-I (gray bars) were driven along ICAM-1–coated surfaces in a laminar flow chamber. The motion of individual cells was monitored (1205 control cells, 414 cells from LAD-III patient, and 692 cells from a patient with LAD-I) for quantitative determination of the number of (*A*) total detectable arrests (duration >200 ms) and (*B*) durable arrests (>1 min duration). Experiments were done in control medium with unstimulated cells, cells that had been incubated in EDTA or stimulated with fMLF (fMLP), PMA, or in medium supplemented with $Mn^{2+}$. Results are expressed in mean (SD). Decrease significant at $*p < 0.05$ and $**p < 0.01$.

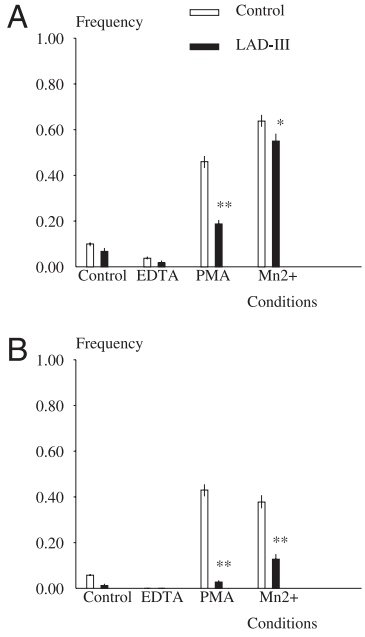


**FIGURE 4.** Lymphocyte adhesion under flow. T lymphocytes from control (white bars) or LAD-III (black bars) were driven along ICAM-1–coated surfaces in a laminar flow chamber. The motion of individual cells was monitored (2229 control cells and 1396 cells from LAD-III) for quantitative determination of the number of (*A*) total detectable arrests (duration >200 ms) and (*B*) durable arrests (>1 min duration). Experiments were done in control medium with unstimulated cells, cells that had been incubated in EDTA or stimulated with fMLF, PMA, or in medium supplemented with $Mn^{2+}$. Results are expressed in mean (SD). Decrease significant at $*p < 0.05$ and $**p < 0.01$.

involved in the attachment strengthening process occurring during the first minute after bond formation.

Because an early and important consequence of lymphocyte adhesion to activating surfaces is the formation within a few minutes of an area of close membrane apposition of the order of several square micrometers (23), we looked for a possible effect of kindlin-3 deficiency on this process.

*Leukocyte spreading*

*Granulocyte spreading.* Purified neutrophils were deposited on surfaces coated with ICAM-1 and subjected to different stimuli (none, fMLF chemoattractant, PMA/ionomycin, $Mn^{2+}$). A quantitative refinement of IRM (22, 23) was used to quantify the area of molecular contact formed 15 min after cell deposition. Typical images are shown on Fig. 5, and quantitative results are summarized on Fig. 6. Control neutrophils displayed substantial spreading in absence of stimulation (mean area, 28 $\mu m^2$) and this displayed, respectively, 3.8-, 5.1-, and 1.6-fold enhancement in presence of fMLF, PMA/ionomycin, or $Mn^{2+}$. However, patient's neutrophils displayed nearly abolished spreading capacity in all conditions excepted after signaling-independent integrin activation with $Mn^{2+}$.

*Lymphocyte spreading.* First, purified T lymphocytes were deposited on ICAM-1–coated surfaces under different conditions of stimulation (none, $Mn^{2+}$, $Mg^{2+}$/EGTA, PMA/ionomycin). Typical images are shown in Fig. 7, and quantitative results are displayed in Fig. 8.

In the absence of stimulation, the contact area formed after 15-min incubation on the ICAM-1–enriched surface was at least 10-fold lower for LAD-III cells than for controls.

Combination of PMA and ionomycin induces full cell activation in agreement with published reports (29) with a strong increase of contact formation by control (~5-fold increase) or patient's cells (8.5-fold), but the latter remained 10-fold lower than "normal" values.

Combining ICAM-1 and CD3 strongly stimulated contact formation for control cells, resulting in an average area that was nearly 10-fold higher than that measured on the patient's lymphocytes.

$Mn^{2+}$ or $Mg^{2+}$/EGTA induced a dramatic (>10-fold) increase of contact measured with patient's cells, but the contact area remained much lower than for controls. This confirmed that patient's integrins were readily activated with an extracellular signal, but contact formation remained defective, whereas bond formation under flow was comparable with that of controls.

Thus, patient lymphocytes displayed a marked spreading defect under all tested conditions. Because spreading involves both adhesive interactions and active cell function, it seemed interesting to know whether patient's cells displayed any activation defect in addition to impaired integrin activation. This question was

Table III. Binding of soluble ICAM-1

| Leukocytes | EDTA-Containing Medium | $Mn^{2+}$-Containing Medium |
|---|---|---|
| Control subject | 435 | 2593 |
| Patient (exp. 1) | 235 | 1437 |
| Patient (exp. 2) | 153 | 1166 |

Blood leukocytes from patient or a control subject (healthy volunteer) were assayed with flow cytometry after incubation with fluorescent anti-human Fc Ig with or without preincubation with soluble Fc-ICAM. Adding manganese resulted in ~6-fold enhancement of median binding as compared with cation-deprived medium. Results of two separate experiments done on patient's cells are shown.

Exp., experiment.

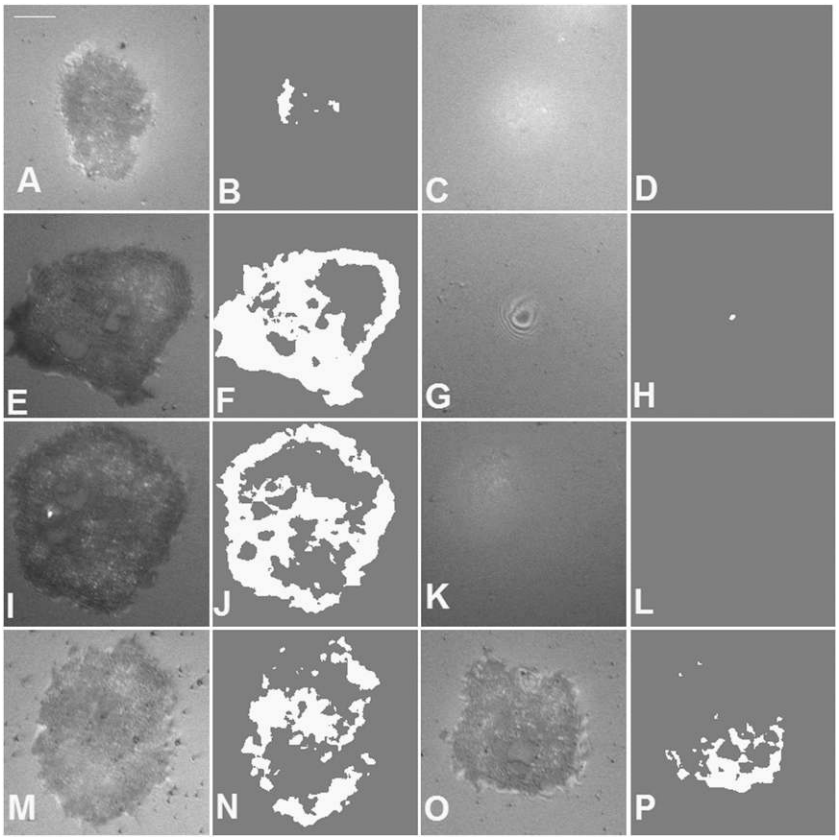


**FIGURE 5.** Neutrophil spreading on ICAM-1–coated surfaces. Neutrophils from healthy volunteers or LAD-III patient were sedimented on ICAM-1–coated surfaces in control medium (*A–D*), or in presence of fMLF (*E–H*), or PMA + ionomycin (*I–L*) or $Mn^{2+}$ (*M–P*) and examined with IRM/RICM 10–15 min later. Typical images are shown together with estimated zone of molecular contact as follows: (*A*, *E*, *I*, *M*) control neutrophils, (*B*, *F*, *J*, *N*) corresponding contact area, (*C*, *G*, *K*, *O*) LAD-III neutrophils, and (*D*, *H*, *L*, *P*) corresponding contact area. Scale bar, 5 μm.

addressed by studying T lymphocyte spreading on cells coated with surfaces that were only adhesive (HLA coated) or both adhesive and activating (anti-CD3 coated) as recently demonstrated (23). Typical images are shown in Fig. 9, and quantitative results are summarized in Fig. 10.

Interestingly, patient's cells formed contact with anti-HLA at least as efficiently as control cells. However, replacing anti-HLA with anti-CD3 resulted in 56% increase of contact area measured with control cells, and only 25% increase of contact area formed with patient's cells, revealing a moderate but highly significant ($p < 0.001$) defect of early spreading of kindlin-3–defective cells deposited on anti-CD3–coated surfaces.

Furthermore, when ICAM-1–coated surfaces were additionally coated with a low (1/100) amount of anti-CD3 Abs, LAD-III cells did not form any substantial contact, whereas control cells formed a low but significant contact.

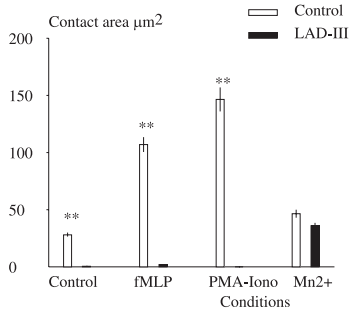


**FIGURE 6.** Quantitative determination of neutrophil spreading on ICAM-1–coated surfaces. The mean contact area formed by neutrophils sedimented on ICAM-1–coated surfaces was determined on control (white bars) and LAD-III (black bars) neutrophils under different conditions as shown. A total of 3824 images of individual cells were processed. Vertical bar length is 2 × SEM. Difference between control and patient's neutrophils is significant at $^{**}p < 0.01$.

### *Expression of an integrin activation epitope after cell stimulation*

Because conformational changes play an important role in integrin activation, we believed it would be interesting to complement functional studies with a study of activation epitopes. We used as an activation reporter mAb 24 that was shown to be specific for some activated conformers of α subunits of $\beta_2$ integrins (17).

*Neutrophils.* As shown in Fig. 11, control neutrophil stimulation with PMA and/or ionomycin and fMLF resulted in moderate (~2-fold) yet significant ($p < 0.01$) increase of mAb 24 epitope expression, whereas nearly 10-fold increase was induced by $Mn^{2+}$. The patient's leukocytes displayed comparable behavior. The only substantial difference was that the binding of mAb 24 was undetectable in absence of stimulation.

*T lymphocytes.* As shown in Fig. 12, patients' and control lymphocytes displayed comparable behavior. Mean fluorescence index was <100 in absence of stimulation, 400–500 after PMA and/or ionomycin stimulation, and >3000 in presence of $Mn^{2+}$.

All these results support the view that kindlin-3 deficiency results in a defect of adhesion strengthening that follows the initial phase of increased accessibility of binding sites. An intriguing point was that patient's cells displayed decreased adhesion on anti-CD3–coated surfaces, a process that is not supposed to involve integrin function.

## Discussion

We have described a new patient with LAD-III, as shown by defective kindlin-3 production, and a combination of immune deficiency and a Glanzmann-type bleeding disease that arise from

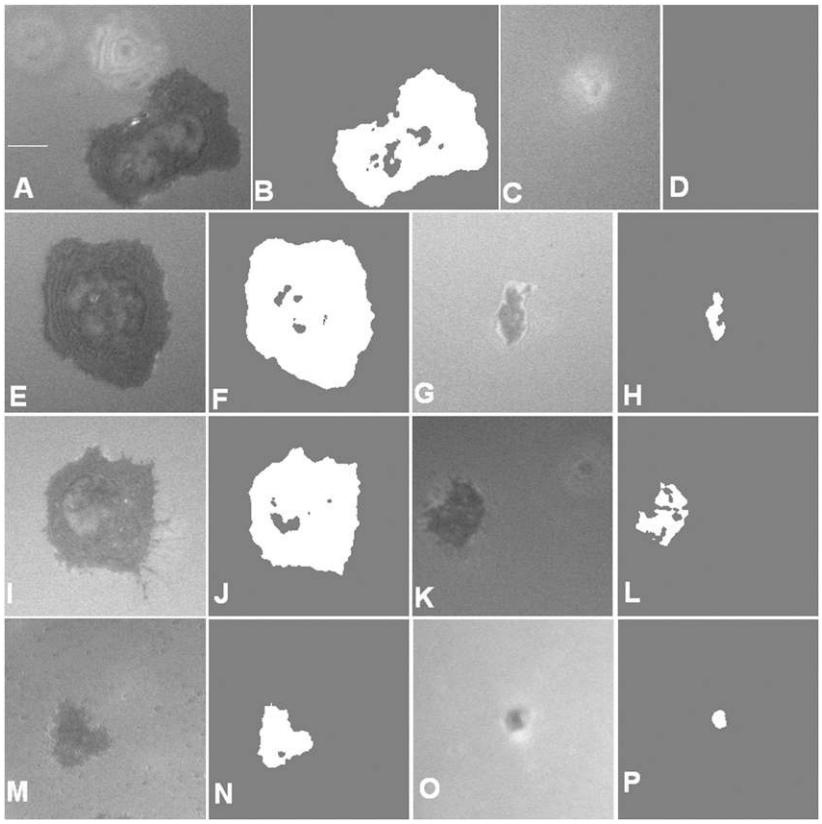


**FIGURE 7.** Lymphocyte spreading on ICAM-1–coated surfaces. T lymphocytes from healthy volunteers or LAD-III patient were sedimented on ICAM-1–coated surfaces in control medium (*A–D*), or in presence of PMA + ionomycin (*E–H*), or on surfaces coated with 1% anti-CD3 in addition to ICAM-1 (*I–L*), or in medium containing $Mn^{2+}$ (*M–P*). Cells were examined with IRM/RICM 10–15 min later. Typical images are shown together with estimated zone of molecular contact as follows: (*A*, *E*, *I*, *M*) control cells, (*B*, *F*, *J*, *N*) corresponding contact area, (*C*, *G*, *K*, *O*) LAD-III cells, and (*D*, *H*, *L*, *P*) corresponding contact area. Scale bar, 5 μm.

abnormal integrin activation. Although strong similarities were found between the nearly 20 LAD-III patients reported to date, some differences are noticeable. The reasons for these differences can be multiple. The majority of the *FERMT3* gene mutations already described was localized in the amino-terminal moiety of the gene, especially in the pleckstrin homology and FERM 3 subdomains. In this article, we report a mutation located in the initial F0 subdomain. A cryptic splice site was used 10 nt downstream from the start of exon 3. We could not exclude that the production of an abnormal protein may modulate cell phenotype, although the decrease in mRNA level may indicate that this mutation results in an unstable transcript.

The phenotype can also be modulated by other genetic and epigenetic modifiers. This is well illustrated by the recent description of two LAD-III siblings (11), only one of whom presented with osteopetrosis, a feature previously described in LAD-III patients but not in the reported case.

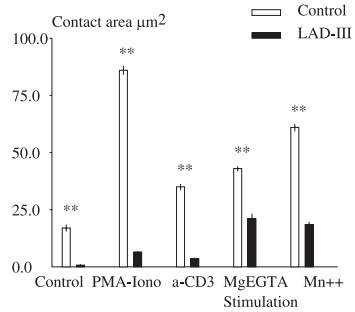


**FIGURE 8.** Quantitative study of T lymphocyte spreading on ICAM-1–coated surfaces. The mean contact area formed by T lymphocytes sedimented on ICAM-1–coated surfaces was determined on control (white bars) and LAD-III (black bars) cells under different conditions as shown. An average of ~500 images of individual cells were processed for each condition. Vertical bar length is 2 × SEM. Difference between control subjects' and patient's neutrophils is significant at $^{**}p < 0.01$.

There is also no accepted set of investigations allowing a dissection of all steps of integrin function. An important goal of this report was to describe adhesion assays allowing us to discriminate between the earliest steps of integrin-mediated leukocyte adhesion. Receptor-mediated cell attachment may be divided into three sequential steps. The first step is the formation of a first molecular bond between a cell and the surface. Because a single ICAM-1/LFA-1 bond could sustain a force of several tens of pN during a period ranging between less than a second and several tens of seconds (30–32), it should generate a detectable event with our experimental setup and therefore be accounted by the total arrest/cell parameter (19). The second step may be described as attachment strengthening as a consequence of formation of additional and durable bonds. This point is significant because surface integrin mobility and/or association with cytoskeletal elements are known to influence functional activity (6–8) in addition to conformational changes. This second step should be accounted for by the durable arrest/cell parameter. The third step is an alignment (22, 33, 34) of the cell membrane along the ligand-coated surface to provide a region of several squared micrometers where surfaces are at binding distance, that is, less than ~40 nm if adhesion is due to LFA-1/ICAM-1 interaction (35). This step proceeds within a few minutes (22) and may be followed by extensive spreading. This was accounted for by the contact area parameter.

Our results allowed the following conclusions: first, chemokine receptor activation with fMLF (neutrophils) or protein kinase C activation with PMA (neutrophils and T lymphocytes) markedly increased initial bond formation (step 1), thus confirming that $\beta_2$ integrins were fairly inactive in resting cells, and that inside-out signaling could activate them at least partially in the absence of kindlin-3. Second, attachment strengthening (step 2) was nearly abolished in PMA-stimulated lymphocytes but not in PMA-

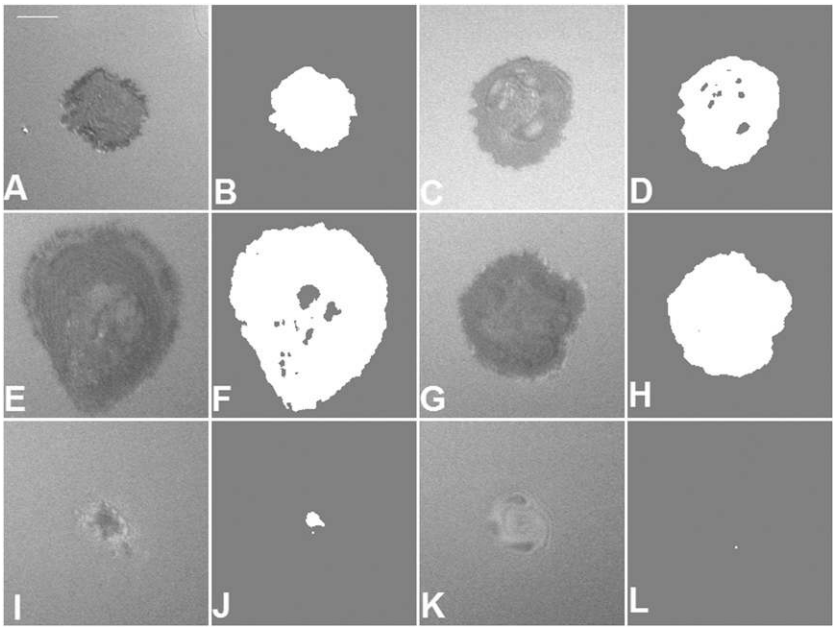


**FIGURE 9.** Lymphocyte spreading on nonstimulating or stimulating adhesive surfaces. T lymphocytes from healthy volunteers or LAD-II patient were sedimented on surfaces coated with anti-HLA (*A–D*), anti-CD3 (*E–H*), or anti-CD3 diluted 1/100 in IgG1 (*I*, *J*). Cells were examined 15 min later with IRM/RICM. Typical images are shown together with estimated zone of molecular contact as follows: (*A*, *E*, *I*) control cells, (*B*, *F*, *J*) corresponding contact area, (*C*, *G*, *K*) LAD-III cells, and (*D*, *H*, *L*) corresponding contact area. Scale bar, 5 μm.

stimulated neutrophils. This finding suggests that kindlin-3 deficiency might be differentially compensated in two different cellular environments. Few studies have documented the effect of PMA on neutrophil functions in kindlin-3–deficient patients. In previously studied patients, $\beta_2$ integrins retained the ability to acquire activation neoepitopes in response to neutrophil stimulation by phorbol ester (14), and NADP oxidase was induced normally by phorbol ester (12). However, Malinin et al. (16) and McDowall et al. (15) reported selective impairment of activation-dependent functions of the neutrophils $\alpha_M\beta_2$ integrin under PMA stimulation. Neutrophils failed to adhere to fibrinogen and did not aggregate. All together, these data and ours may indicate differences in the protein kinase C/kindling-3/$\beta_2$ integrins connections in neutrophils depending on which heterodimer is engaged, LFA-1 ($\alpha_L\beta_2$) or Mac-1 ($\alpha_M\beta_2$), as well as differences in intracellular signaling cascades (4).

Third, we showed an abnormal early spreading of T lymphocytes on adhesive surfaces. Results confirmed the incomplete restoration of integrin function after PMA stimulation, because the contact area formed by patient's lymphocytes on ICAM-1–coated surfaces after PMA stimulation was >10-fold lower than that of controls. This was not due to an intrinsic spreading deficiency, because spreading on anti-HLA was not decreased in patient's cells. In contrast, spreading on anti-CD3–coated surfaces was slightly (~36%) but significantly lower in patient's cells as compared with control cells. This defect was confirmed when cells were deposited on surfaces coated with low amounts of anti-CD3: the low contact formation found on control cells was completely abolished on cells from the patient. Because no integrin ligand was involved in this function, results strongly suggest that kindlin-3–defective lymphocytes displayed a spreading defect independent of ligand recognition by integrins. Although more work is needed to interpret this finding, this is consistent with preliminary data supporting the capacity of kindlin-3 to interact with microfilaments through migfilin and filamin (16). Also, it is now well recognized that there is a substantial overlap between integrin- and TCR-triggered signaling (29). Accordingly, LFA-1 was recently reported to influence T cell activation in a ligand-independent way (36). In addition, achieving unambiguous discrimination between inside-out and outside-in LFA-1 signaling is made still more difficult by the well-recognized difficulty of measuring the cell capacity to bind soluble ICAM-1 ligand (37), and the dependence of integrin function on both conformation-dependent and

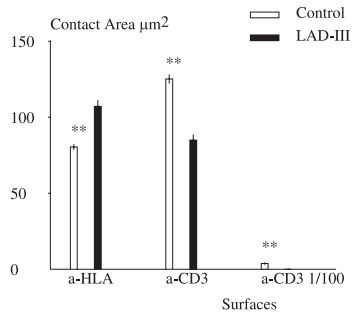


**FIGURE 10.** Quantitative study of T lymphocyte spreading on nonstimulating or stimulating adhesive surfaces. The mean contact area formed by T lymphocytes sedimented on Ab-coated surfaces was determined on control (white bars) and LAD-III (black bars) cells under different conditions as shown. An average of ~500 images of individual cells was processed for each condition. Vertical bar length is 2 × SEM. Difference between control subjects' and patient's neutrophils is significant at $^{**}p < 0.01$.

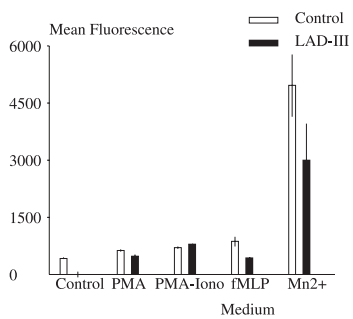


**FIGURE 11.** Induction of an integrin activation epitope on stimulated neutrophils. The uptake of mAb 24 was measured on control (white bars) or LAD-III (black bars) neutrophils under different conditions as shown. Mean fluorescence was determined. Average of two to six different determinations is shown. Vertical bar length is 2 × SEM. No significant difference was found between control and patient cells.

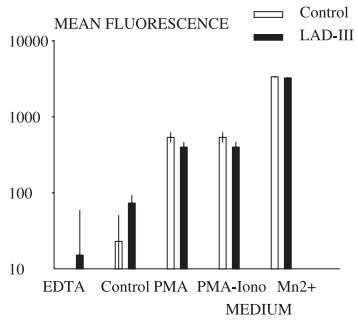


**FIGURE 12.** Induction of an integrin activation epitope on stimulated lymphocytes. The uptake of mAb 24 was measured on control (white bars) or LAD-III (black bars) neutrophils under different conditions as shown. Mean fluorescence was determined. Average of two to six different determinations is shown. Vertical bar length is 2 × SEM. No significant difference was found between control and patient cells.

-independent mechanisms (38). Thus, the lymphocyte proliferation defect found in previous studies (12) and our report might be ascribed either to an integrin-independent process or to a possible role of LFA-1/ICAM-1 interaction in enhancing lymphocyte proliferation through intercellular aggregation processes.

Results obtained with mAb 24 are also compatible with binding data. Indeed, although a high and comparable increase of 24 epitope expression was found after $Mn^{2+}$ treatment of patient's and control cells, as expected, the moderate but significant increase of 24 epitope expression found in stimulated patient's cells was compatible with the increased initial binding measured with the flow chamber.

In conclusion, despite an impressive amount of recent information, integrin-mediated adhesion and the particular role of kindlins in this process remain incompletely understood. It is suggested that a combination of a better dissection of the functional steps of adhesion and a study of patients with specific deficiencies will help to more completely unravel the mechanisms involved in cell adhesion processes.

## Acknowledgments

We thank N. Saut (Laboratoire d'Hématologie, Hôpital de la Timone, Assistance Publique-Hôpitaux de Marseille) for gene sequencing, D. Touchard (INSERM U600) for analysis of IRM images, and L. Chiche (Service Médecine Interne, Hôpital de la Conception, Marseille) for helpful discussion. A.T.N. acknowledges the role of R. Heilig (Genoscope, Evry), M. Fiore, and X. Pillois (Centre de Recherche Paul Pascal, Bordeaux) in the ITGA2B gene sequencing.

## Disclosures

The authors have no financial conflicts of interest.

## References

1. Shattil, S. J., C. Kim, and M. H. Ginsberg. 2010. The final steps of integrin activation: the end game. *Nat. Rev. Mol. Cell Biol.* 11: 288–300.
2. Ley, K., C. Laudanna, M. I. Cybulsky, and S. Nourshargh. 2007. Getting to the site of inflammation: the leukocyte adhesion cascade updated. *Nat. Rev. Immunol.* 7: 678–689.
3. Coller, B. S., and S. J. Shattil. 2008. The GPIIb/IIIa (integrin alphaIIbbeta3) odyssey: a technology-driven saga of a receptor with twists, turns, and even a bend. *Blood* 112: 3011–3025.
4. Abram, C. L., and C. A. Lowell. 2009. The ins and outs of leukocyte integrin signaling. *Annu. Rev. Immunol.* 27: 339–362.
5. van Kooyk, Y., P. Weder, K. Heije, and C. G. Figdor. 1994. Extracellular Ca2+ modulates leukocyte function-associated antigen-1 cell surface distribution on T lymphocytes and consequently affects cell adhesion. *J. Cell Biol.* 124: 1061–1070.
6. Lub, M., Y. van Kooyk, S. J. van Vliet, and C. G. Figdor. 1997. Dual role of the actin cytoskeleton in regulating cell adhesion mediated by the integrin lymphocyte function-associated molecule-1. *Mol. Biol. Cell* 8: 341–351.
7. Kucik, D. F., M. L. Dustin, J. M. Miller, and E. J. Brown. 1996. Adhesion-activating phorbol ester increases the mobility of leukocyte integrin LFA-1 in cultured lymphocytes. *J. Clin. Invest.* 97: 2139–2144.
8. Stewart, M. P., A. McDowall, and N. Hogg. 1998. LFA-1-mediated adhesion is regulated by cytoskeletal restraint and by a Ca2+-dependent protease, calpain. *J. Cell Biol.* 140: 699–707.
9. Hynes, R. O. 2002. Integrins: bidirectional, allosteric signaling machines. *Cell* 110: 673–687.
10. Zaidel-Bar, R., S. Itzkovitz, A. Ma'ayan, R. Iyengar, and B. Geiger. 2007. Functional atlas of the integrin adhesome. *Nat. Cell Biol.* 9: 858–867.
11. Jurk, K., A. S. Schulz, B. E. Kehrel, D. Räpple, H. Schulze, D. Möbest, W. W. Friedrich, H. Omran, E. Deak, R. Henschler, et al. 2010. Novel integrin-dependent platelet malfunction in siblings with leukocyte adhesion deficiency-III (LAD-III) caused by a point mutation in *FERMT3*. *Thromb. Haemost.* 103: 1053–1064.
12. Kuijpers, T. W., R. A. Van Lier, D. Hamann, M. de Boer, L. Y. Thung, R. S. Weening, A. J. Verhoeven, and D. Roos. 1997. Leukocyte adhesion deficiency type 1 (LAD-1)/variant. A novel immunodeficiency syndrome characterized by dysfunctional beta2 integrins. *J. Clin. Invest.* 100: 1725–1733.
13. Svensson, L., K. Howarth, A. McDowall, I. Patzak, R. Evans, S. Ussar, M. Moser, A. Metin, M. Fried, I. Tomlinson, and N. Hogg. 2009. Leukocyte adhesion deficiency-III is caused by mutations in KINDLIN3 affecting integrin activation. *Nat. Med.* 15: 306–312.
14. Alon, R., M. Aker, S. Feigelson, M. Sokolovsky-Eisenberg, D. E. Staunton, G. Cinamon, V. Grabovsky, R. Shamri, and A. Etzioni. 2003. A novel genetic leukocyte adhesion deficiency in subsecond triggering of integrin avidity by endothelial chemokines results in impaired leukocyte arrest on vascular endothelium under shear flow. *Blood* 101: 4437–4445.
15. McDowall, A., L. Svensson, P. Stanley, I. Patzak, P. Chakravarty, K. Howarth, H. Sabnis, M. Briones, and N. Hogg. 2010. Two mutations in the *KINDLIN3* gene of a new leukocyte adhesion deficiency III patient reveal distinct effects on leukocyte function in vitro. *Blood* 115: 4834–4842.
16. Malinin, N. L., L. Zhang, J. Choi, A. Ciocea, O. Razorenova, Y. Q. Ma, E. A. Podrez, M. Tosi, D. P. Lennon, A. I. Caplan, et al. 2009. A point mutation in KINDLIN3 ablates activation of three integrin subfamilies in humans. *Nat. Med.* 15: 313–318.
17. Dransfield, I., C. Cabañas, A. Craig, and N. Hogg. 1992. Divalent cation regulation of the function of the leukocyte integrin LFA-1. *J. Cell Biol.* 116: 219–226.
18. Martin, C., X. Viviand, P. Bongrand, L. Papazian, P. Saux, and F. Gouin. 1997. Study of some phagocyte membrane receptors in patients receiving intravenous polyvalent immunoglobulins as adjunct treatment for nosocomial pneumonia. *J. Crit. Care* 12: 193–199.
19. Pierres, A., A. M. Benoliel, and P. Bongrand. 2008. Studying molecular interactions at the single bond level with a laminar flow chamber. *Cell. Mol. Bioeng.* 1: 247–262.
20. Robert, P., K. Sengupta, P. H. Puech, P. Bongrand, and L. Limozin. 2008. Tuning the formation and rupture of single ligand-receptor bonds by hyaluronan-induced repulsion. *Biophys. J.* 95: 3999–4012.
21. Pierres, A., O. Tissot, B. Malissen, and P. Bongrand. 1994. Dynamic adhesion of CD8-positive cells to antibody-coated surfaces: the initial step is independent of microfilaments and intracellular domains of cell-binding molecules. *J. Cell Biol.* 125: 945–953.
22. Pierres, A., P. Eymeric, E. Baloche, D. Touchard, A. M. Benoliel, and P. Bongrand. 2003. Cell membrane alignment along adhesive surfaces: contribution of active and passive cell processes. *Biophys. J.* 84: 2058–2070.
23. Cretel, E., D. Touchard, P. Bongrand, and A. Pierres. 2011. A new method for rapid detection of T lymphocyte decision to proliferate after encountering activating surfaces. *J. Immunol. Methods* 364: 33–39.
24. Snedecor, G. W., and W. G. Cochran. 1980. *Statistical Methods.* Iowa University Press, Ames, IA, p. 124–126.
25. George, J. N., J. P. Caen, and A. T. Nurden. 1990. Glanzmann's thrombasthenia: the spectrum of clinical disease. *Blood* 75: 1383–1395.
26. Schlegel, N., O. Gayet, M. C. Morel-Kopp, B. Wyler, M. F. Hurtaud-Roux, C. Kaplan, and J. Mc Gregor. 1995. The molecular genetic basis of Glanzmann's thrombasthenia in a gypsy population in France: identification of a new mutation on the alpha IIb gene. *Blood* 86: 977–982.
27. Kuijpers, T. W., E. van de Vijver, M. A. J. Weterman, M. de Boer, A. T. J. Tool, T. K. van den Berg, M. Moser, M. E. Jakobs, K. Seeger, O. Sanal, et al. 2009. LAD-1/variant syndrome is caused by mutations in *FERMT3*. *Blood* 113: 4740–4746.
28. Pierres, A., A. M. Benoliel, and P. Bongrand. 1996. Measuring bonds between surface-associated molecules. *J. Immunol. Methods* 196: 105–120.
29. Smith-Garvin, J. E., G. A. Koretzky, and M. S. Jordan. 2009. T cell activation. *Annu. Rev. Immunol.* 27: 591–619.
30. Evans, E., K. Kinoshita, S. Simon, and A. Leung. 2010. Long-lived, high-strength states of ICAM-1 bonds to beta2 integrin, I: lifetimes of bonds to recombinant alphaLbeta2 under force. *Biophys. J.* 98: 1458–1466.
31. Vitte, J., A. M. Benoliel, P. Eymeric, P. Bongrand, and A. Pierres. 2004. Beta-1 integrin-mediated adhesion may be initiated by multiple incomplete bonds, thus accounting for the functional importance of receptor clustering. *Biophys. J.* 86: 4059–4074.

32. Zhang, X., E. Wojcikiewicz, and V. T. Moy. 2002. Force spectroscopy of the leukocyte function-associated antigen-1/intercellular adhesion molecule-1 interaction. *Biophys. J.* 83: 2270–2279.
33. Pierres, A., A. M. Benoliel, D. Touchard, and P. Bongrand. 2008. How cells tiptoe on adhesive surfaces before sticking. *Biophys. J.* 94: 4114–4122.
34. Dustin, M. L. 1997. Adhesive bond dynamics in contacts between T lymphocytes and glass-supported planar bilayers reconstituted with the immunoglobulin-related adhesion molecule CD58. *J. Biol. Chem.* 272: 15782–15788.
35. Springer, T. A. 1990. Adhesion receptors of the immune system. *Nature* 346: 425–434.
36. Li, D., J. J. Molldrem, and Q. Ma. 2009. LFA-1 regulates CD8+ T cell activation via T cell receptor-mediated and LFA-1-mediated Erk1/2 signal pathways. *J. Biol. Chem.* 284: 21001–21010.
37. Feigelson, S. W., R. Pasvolsky, S. Cemerski, Z. Shulman, V. Grabovsky, T. Ilani, A. Sagiv, F. Lemaître, C. Laudanna, A. S. Shaw, and R. Alon. 2010. Occupancy of lymphocyte LFA-1 by surface-immobilized ICAM-1 is critical for TCR- but not for chemokine-triggered LFA-1 conversion to an open headpiece high-affinity state. *J. Immunol.* 185: 7394–7404.
38. Vitte, J., A.-M. Benoliel, A. Pierres, and P. Bongrand. 2005. Regulation of cell adhesion. *Clin. Hemorheol. Microcirc.* 33: 167–188.